전력전자학술대회 논문집 2003. 7. 14 ~ 7. 17

이중권선 유도발전기로 구동되는 유도전동기의 수동성기반제어기 설계

이상철, 김종현
한국전기연구원

Passivity-based Controller Design for Induction Motor Driven by Doubly-fed Induction Generator

S.C. Lee and J.H. Kim
Korea Eletrotechnology Research Institute (KERI)

ABSTRACT

We are interested in this paper on the control of an electromechanical system consisting of a doubly-fed induction generator(DFIG), driven by a prime mover that can supply or extract mechanical power, e.g., a flywheel inertia, and an induction motor(IM). The stator of the induction machine is connected to the stator of the generator whose rotor voltage is regulated by a bidirectional converter. The main interest of this configuration is that it permits a bidirectional power flow between the motor, which may operate in regenerative mode, and the generator. We propose a passivity-based controller to regulate the motor mechanical speed. Since this kind of controllers achieve stabilization via energy balancing, regulation of the power flow in the system is naturally incorporated. Simulation results are presented to illustrate the main points of our paper.

1. Introduction

The doubly-fed induction generator(DFIG) can supply power at constant voltage and constant frequency while the rotor speed varies. This makes it suitable for variable speed wind energy applications. Additionally, when a bidirectional AC-AC converter is used in the rotor circuit, the speed range can be extended above synchronous speed and power can be generated both from the stator and the rotor. An advantage of this type of DFIG drive is that the rotor converter need only rated for a fraction of the total output power, the fraction depending on the allowable sub- and super-synchronous speed range. A good introduction to the operational characteristic of the DFIG connected to the grid can be found in [1].

The possibility of a DFIG supplying an isolated load has been indicated [2],[3] in which some mention is made of the steady state control problem. In [4] a system is presented in which the rotor is supplied from a battery via a PWM converter with experimental results from a 250W prototype. A control system based on regulating the rms voltage is used which results in large voltage deviations and very slow recovery following load changes. See also [8],[9] where feedback linearization and sliding mode principles are used for the design of motor speed controllers.

The present paper constitutes a first, if modest, attempt to use energy principles to regulate the dynamic operation of this bidirectional power flow system. For, we propose a standard passivity-based control(PBC)[5] to regulate the motor mechanical speed. Since PBC achieves stabilization via energy-balancing, the task of regulating the power flow in the system is naturally incorporated. In standard PBC we a priori select the storage function to be assigned(typically quadratic in the increments) and then design the controller that renders the storage function nonincreasing. This approach, clearly reminiscent of standard Lyapunov methods, has been very successful to control physical systems described by Euler-Lagrange equations of motion, which is thoroughly detailed in [5].

This paper presents a isolation operation of DFIG supplying an induction motor to control speed and torque. System modeling and stability analysis are performed with the passivity-based control(PBC) scheme[5]. Also, performance of the proposed controller

is verified through simulation studies.

2. System Configuration

DFIG has been used to convert mechanical power into electrical power operating near the synchronous speed with some advantages over the synchronous or squirrel cage generators. These advantages are the high overall efficiency of the system and the low power of the converter, which is in the rotor of the machine.[6],[7],[8] In the isolated operation, the stator of the DFIG is connected to a load, in this case an induction motor(IM), obtaining a variable frequency/variable voltage(VVVF) operation. Fig.1 shows the configuration of this system. If the DFIG is driven by a constant speed prime mover, this generation scheme can be used for example in several autonomous generation plants. With the prime mover running at constant speed, the performance of the primary energy source can be optimized.

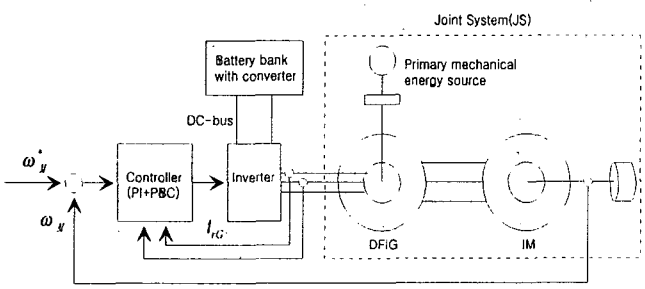

Fig. 1 System configuration with controller

The behavior of the joint system(JS) can be explained as follows : JS is an autonomous generation system that can drive a rotating load with mechanical speed w_M and torque τ_M, delivering an output power to the load. JS is operated by the prime mover or a gas turbine, depending on the type of isolated plant considered. Prime mover maintains a constant mechanical speed $w_M = K$, where K is chosen to optimize global performance. A bank of batteries is connected to the JS rotor circuit via a converter, delivering slip power which is a fraction of total power.

3. Dynamic Equation of DFIG with IM

The joint system consists of a wound rotor generator(DFIG) with a squirrel cage motor(IM), which are connected at each stator windings. Ideal symmetrical phases and sinusoidally distributed phase windings are assumed. The permeability of the fully laminated cores is assumed to be infinite, and saturation, iron losses, end winding and slot effects are neglected. Only linear magnetic materials are considered, and it is further assumed that all parameters are constant and known. The equivalent circuit is shown in Fig.2 and the signal names are described. Note that subscripts G and M mean generator and motor, respectively.

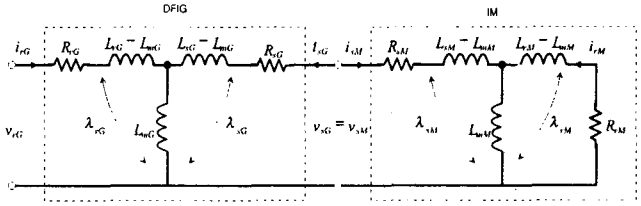

Fig. 2 Equivalent circuit of the DFIG with IM

The standard two phase of an n_G pole pairs DFIG with uniform air-gap can be formulated :

$$\dot{\lambda}_{sG} + R_{sG} i_{sG} = v_{sG} \tag{1}$$

$$\dot{\lambda}_{rG} + R_{rG} i_{rG} = v_{rG} \tag{2}$$

and n_M for IM :

$$\dot{\lambda}_{sM} + R_{sM} i_{sM} = v_{sM} \tag{3}$$

$$\dot{\lambda}_{rM} + R_{rM} i_{rM} = 0. \tag{4}$$

After connecting stator windings together, the current and voltage constraints are given

$$v_{sG} = v_{sM}, \quad i_{sG} = -i_{sM}. \tag{5}$$

Applying (5) to (2) and (4), the following system equations are calculated

$$\Sigma_e : \dot{\lambda} + Ri = \begin{bmatrix} I_2 \\ 0 \end{bmatrix} = Mu \tag{6}$$

where, flux vector is defined by $\lambda = [\lambda_{rG} \ \lambda_{sGM} \ \lambda_{rM}]^T = [\lambda_{rG} \ \lambda_{sG} - \lambda_{sM} \ \lambda_{rM}]^T$ and current vector by $i = [i_{rG} \ i_{sG} \ i_{rM}]^T$. The inductance matrix can transform current to flux with the relationship $\lambda = L(\theta) i$,

$$\begin{bmatrix} L_{rG} I_2 & L_{mG} e^{-Jn_G \theta_G} & 0 \\ L_{mG} e^{Jn_G \theta_G} & (L_{sG} + L_{sM}) I_2 & -L_{mM} e^{Jn_M \theta_M} \\ 0 & -L_{mM} e^{-Jn_M \theta_M} & L_{rM} I_2 \end{bmatrix}$$

and resistance matrix is described by $R = diag\{R_{rG} I_2, (R_{sG} + R_{sM}) I_2, R_{rM} I_2\}$. The input vector is defined by $u = v_{rG}$. L_{sG}, L_{rG}, L_{mG} are the stator, rotor, and mutual inductances for DFIG and

L_{sM}, L_{rM}, L_{mM} for IM, respectively. R_{sG}, R_{rG} are stator and rotor resistances for DFIG and R_{sM}, R_{rM} for IM, respectively. θ_G is the rotor position with respect to stator for DFIG and θ_M for IM. Some matrices and their properties are summarized as

$$J = \begin{bmatrix} 0 & -1 \\ 1 & 0 \end{bmatrix} = -J^T, I_2 = \begin{bmatrix} 1 & 0 \\ 0 & 1 \end{bmatrix} \quad (8)$$

$$e^{J\theta} = \begin{bmatrix} \cos(\theta) & -\sin(\theta) \\ \sin(\theta) & \cos(\theta) \end{bmatrix} = (e^{-J\theta})^T$$

$$Je^{J\theta} = e^{J\theta}J. \quad (9)$$

The mechanical dynamics are given

$$\Sigma_m: J_m\dot{\omega}_m + B_m\omega_m = \tau - \tau_L \quad (10)$$

where, generated torques are calculated from differentiating the system energy function with respect to mechanical positions $\theta = [\theta_G \ \theta_M]^T$

$$\begin{aligned} \tau &= \begin{bmatrix} \tau_G \\ \tau_M \end{bmatrix} = \frac{1}{2}\frac{\partial}{\partial\theta} i^T L(\theta) i \\ &= \frac{\partial}{\partial\theta}\left(L_{mG} i_{rG}^T e^{-Jn_G\theta_G} i_{sG} - L_{mM} i_{sG}^T e^{Jn_M\theta_M} i_{rM}\right) \\ &= \begin{bmatrix} -L_{mG} i_{rG}^T e^{-Jn_G\theta_G} i_{sG} \\ -L_{mM} i_{sG}^T e^{Jn_M\theta_M} i_{rM} \end{bmatrix} \\ &= \begin{bmatrix} -\frac{n_G}{R_{sG}} + R_{sM}\lambda_{sGM}^T J\left(\lambda_{sGM} - L_{mM} e^{Jn_M\theta_M} i_{rM}\right) \\ \frac{n_M}{R_{rM}} \lambda_{rM}^T J \lambda_{rM} \end{bmatrix}. \end{aligned}$$

Mechanical inertia matrix is $J_m = diag\{J_G, J_M\}$, and damping coefficient matrix $B_m = diag\{B_G, B_M\}$. J_G, B_G are mechanical inertia and damping coefficient for DFIG; J_M, B_M are mechanical inertia and damping coefficient for IM. Mechanical rotor speeds are denoted by $\omega_m = [\omega_G \ \omega_M]^T$.

4. Nested-loop PBC for speed-torque tracking

A feedback decomposition approach[5] for the design of a torque tracking PBC is adopted here. In this section we solve the speed tracking problem posed above by adding an outer-loop controller to this torque tracking PBC. This leads to the nested-loop(i.q. cascaded) scheme depicted in Fig.4, where C_{il} is the inner-loop torque tracking PBC and C_{ol} is an outer-loop speed controller, which generates the desired torque. C_{ol} may be taken as PI controller. Now we derive the torque tracking PBC from the perspective of systems "inversion". The derivation is easier to understand if the flux vector is used in the calculations instead of the current vector. The proposed PBC is a "copy" of the electrical dynamics of the motor (6) with an additional damping injection term introduced to get strict passivity. In the implicit form, this yields

$$M = \dot{\lambda}^d + RL^{-1}(\theta)\lambda^d + K(\omega_m)L^{-1}(\theta)\tilde{\lambda} \quad (11)$$

$$\tau_M^d = \frac{n_M}{R_{rM}} \lambda^{dT_{rM}} J \lambda^{d}{}_{rM} \quad (12)$$

where $\tilde{\lambda} = \lambda - \lambda^d$ and superscript d means the desired value. Notice that the damping injection $K(\omega_m)$ is independent on θ.

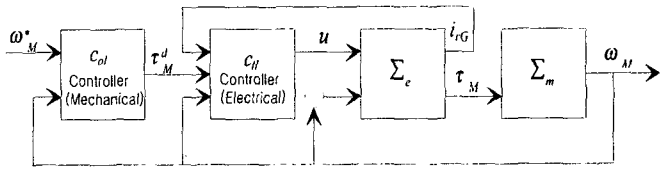

Fig. 3 Nested-loop control configuration

Let us now analyze the stability of the closed-loop. The error equation for the fluxes is obtained from (6) and (11) as

$$\dot{\tilde{\lambda}} + (R + K)L^{-1}(\theta)\tilde{\lambda} = 0. \quad (13)$$

We will show now that it is also possible to prove convergence, even without the damping injection. To this end, consider the storage function

$$H = \frac{1}{2}\tilde{\lambda}^T R^{-1}\tilde{\lambda} \geq 0 \quad (14)$$

whose derivative satisfies

$$\dot{H} = -\tilde{\lambda}^T L^{-1}(\theta)\tilde{\lambda} \leq -\alpha H \quad (15)$$

$\alpha > 0$ for some . Hence, $\tilde{\lambda} \to 0$ exponentially fast. It is easy to see that the closed-loop equations define an output strictly passive with storage function H. Global convergence of $\tilde{i}$ to zero is established with $\tilde{i} = L^{-1}(\theta)\tilde{\lambda}$.

To illustrate the second difficulty in the stability analysis of the nested-loop scheme, let us turn out attention to the torque tracking error $\tilde{\tau}_M = \tau_M - \tau_M^d$. After some simple operation from (10) and (12) we get

$$\begin{aligned} \tilde{\tau}_M &= \frac{n_M}{R_{rM}} \tilde{\lambda}^{T_{rM}} J \lambda_{rM} + \lambda^{dT_{rM}} J \tilde{\lambda}_{rM} \\ &= n_M - \tilde{i}^{T_{rM}} J \lambda_{rM} + \frac{1}{R_{rM}} \lambda^{dT_{rM}} J \tilde{\lambda}_{rM} \end{aligned} \quad (16)$$

where we have used $\tilde{i}_{rM} = -\tilde{\lambda}_{rM}/R_{rM}$. In the torque control problem we assumed that the external

reference τ^d_M and its derivative $\dot{\tau}^d_M$ were bounded, and convergence of $\tilde{\tau}\to 0$ was proved as follows. First, λ^d_{rM} and $\dot{\lambda}^d_{rM}$ are bounded by construction. Then, we have shown above that exponentially convergence $\tilde{\lambda}_{rM}\to 0$, consequently also $\tilde{i}_{rM}\to 0$ and λ_{rM} is bounded. From here we conclude that $\tilde{\tau}_M\to 0$. In speed control τ^d_M and its derivative $\dot{\tau}^d_M$ are generated by outer-loop PI controller, so they can be taken to be bounded.

4.1 Explicit controller form

An explicit realization is obtained by "inversion of" (12)

$$\dot{\lambda}^d_{rM} = \frac{1}{\beta^2_*(t)}\left(R_{rM}\frac{\tau^d_M}{n_M}J + \dot{\beta}_*(t)\beta_*(t)I_2\right)\lambda^d_{rM}$$

$$\lambda^d_{rM}(0) = \begin{bmatrix}\beta_*(0)\\ 0\end{bmatrix} \tag{17}$$

which can actually be solved as

$$\lambda^d_{rM} = e^{J\rho}\begin{bmatrix}\beta_*(t)\\ 0\end{bmatrix}$$

$$\dot{\rho} = \frac{R_{rM}\tau^d_M}{n_M\beta^2_*(t)}, \quad \rho(0)=0. \tag{18}$$

The stator and rotor currents of IM can be calculated with λ^d_{rM},

$$i^d_{rM} = -\frac{1}{R_{rM}}\dot{\lambda}^d_{rM} = -\frac{\tau^d_M}{n_M}\beta^2_*(t)J\lambda^d_{rM} \tag{19}$$

$$i^d_{sM} = \frac{e^{Jn_M\theta_M}}{L_{mM}}\left(I_2 + L_{rM}\frac{\tau^d_M}{n_M}\beta^2_*(t)J\right)\lambda^d_{rM} = -i^d_{sG} \tag{20}$$

where $\beta_*(t)$ is kept as a constant such that $\dot{\beta}_*(t) = 0$.

Next, integral operation of stator current of DFIG results in the difference between DFIG and IM stator fluxes

$$\lambda^d_{sGM} = \lambda^d_{sG} - \lambda^d_{sM} = -(R_{sG}+R_{sM})\int i^d_{sG}\,dt. \tag{21}$$

It is possible to get i^d_{rG} and λ^d_{rG} with already obtained i^d_{rM}, i^d_{sG}, and λ^d_{sGM},

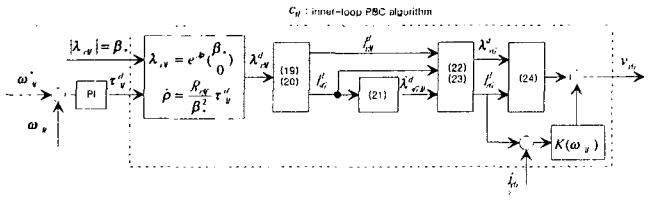

Fig. 4 The explicit form of passivity-based controller.

$$i^d_{rG} = \frac{e^{-Jn_G\theta_G}}{L_{mG}}\left(\lambda^d_{sGM} - (L_{sG}+L_{sM})i^d_{sG} + L_{mM}e^{Jn_M\theta_M}i^d_{rM}\right) \tag{22}$$

$$\lambda^d_{rG} = L_{rG}i^d_{rG} + L_{mG}e^{-Jn_G\theta_G}i^d_{sG}. \tag{23}$$

Finally, the control input voltage can be constructed

$$v_{rG} = \dot{\lambda}^d_{rG} + R_{rG}i^d_{rG} + K\tilde{i}_{rG}. \tag{24}$$

The explicit form of passivity-based controller for torque tracking and outer-loop PI controller for speed tracking is shown in Fig. 3.

5. Simulation Results

Simulation studies are performed utilizing MATLAB/SIMULINK[10]. During transient state, the desired motor current can be high if we use (21), in order to reduce its value (only in transient state) this equation has been changed in $\lambda^d_{sGM} = -\frac{R_{sG}+R_{sM}}{s+\sigma}i^d_{sG}$, where σ is a constant (=10 in this simulation) which is decreased during few iteration in order to get pure integrator.

Firstly, the voltage input at DFIG rotor side is shown in Fig. 5, which is within reasonable range. The DFIG is maintained at constant speed 1000rpm by primer mover system, which is modeled by PI speed controller in simulation program. Secondly, the currents and fluxes of DFIG and IM are shown in Fig. 6 and Fig. 7 respectively. Rotor flux magnitude of motor is chosen as 0.04Wb and it is well regulated as shown in Fig. 7(c). Finally, the speed and torque responses are shown in Fig. 8. Rotor speed reference for IM is 1500rpm and load torque is applied at 1.6 sec with 1 Nm.

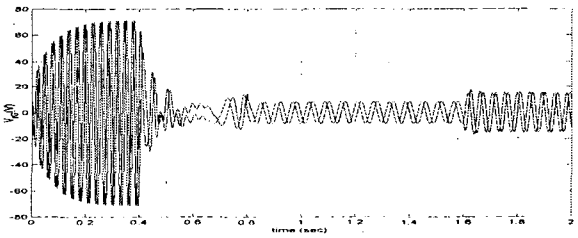

Fig. 5 Input voltage at DFIG rotor winding

6. Conclusion

The speed-torque tracking controller for induction motor powered by DFIG has been

presented. The joint system obtains energy from a primary mechanical source. The DFIG allows to transform this energy but also to control the torque and speed of the induction motor making use of the rotor voltage of DFIG as control variable. Compared with scalar control and feedback linearization control, the proposed passivity-based control algorithm shows successful control performance which is supported with simulation results. For other application of DFIG, such as wind turbine system, speed control of generator is required to capture maximum mechanical energy.

참 고 문 헌

[1] W. Leonhard, "Control of electrical drives", Spring-Verlag, 1985.

[2] M.S. Vicatos and J.A. Tagopoulos, "Steady state analysis of a doubly-fed induction generator under sychronous operation", IEEE Trans. on Energy Conversion, Vol. 4, No. 3, pp. 495-501, 1989.

[3] F. Bogalecka, "Dynamics of the power control of a double fed induction generator connected to the soft power grid", ISIE, Budapest, pp. 509-513, 1993.

[4] A. Mebarky and R.T. Lipczynsky, "'Novel variable speed constant frequency generation system with voltage regualtion", EPE, vol. 2, pp. 465-471, 1995.

[5] R. Ortega, A. Loria, P.J. Nicklasson, and H. Sira-Ramirez, "Passivity-based control of Euler -Lagrange systems", in Communications and Control Engineering. Berlin,Germany: Spring-Verlag, 1998.

[6] R. Datta and V.T. Ranganathan, "Variable-speed wind power generation using doubly fed wound rotor induction machine-a comparision with alternative schemes", IEEE Trans. on energy conversion, vol. 17, no. 3, pp. 414-421, 2002.

[7] S. Muller, M. Deicke, and Rik W. De Doncker, "Doubly fed induction generator systems for wind turbines", IEEE Industry Applications Magazine, vol., no., pp. 26-33, May/June, 2002.

[8] P. Caratozzole, E. Fossas, and J. Riera, "Nonlinear control of an isolated motion system with DFIG", IFAC, 2002.

[9] P. Caratozzole, E. Fossas, and J. Riera, "Robust nonlinear control of an isolated motion system", CIEP, Mexico, 2002.

[10] SIMULINK with MATLAB, The MathWorks, Inc.

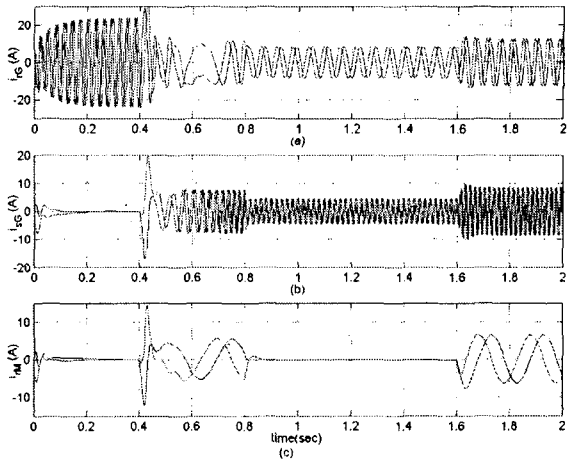

Fig. 6 Currents at (a) DFIG rotor winding, (b) DFIG stator winding, and (c) IM rotor winding.

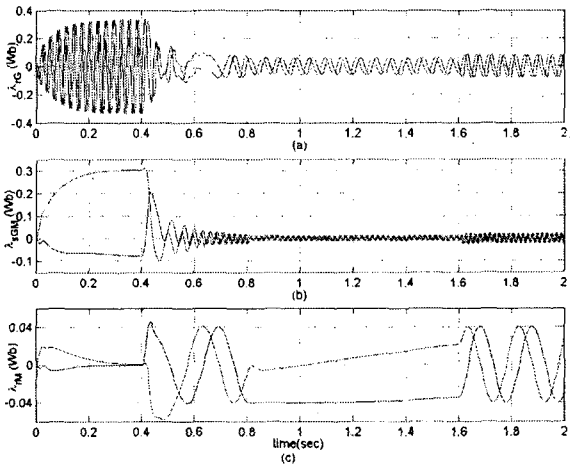

Fig. 7 Fluxes at (a) DFIG rotor winding, (b) DFIG stator connected with IM stator winding, and (c) IM rotor winding.

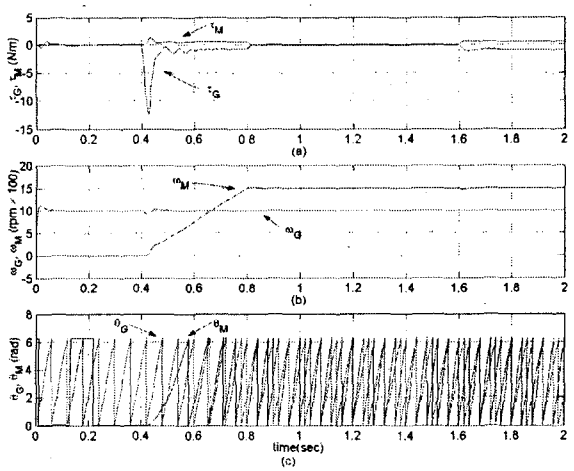

Fig. 8 Mechanical responses : (a) Generated torques, (b) rotor speeds, and (c) rotor positions of DFIG and IM, respectively.